PCCP

Accepted Manuscript

ROYAL SOCIETY OF CHEMISTRY

www.rsc.org/pccp

Journal Name

ARTICLE TYPE

Cite this: DOI: 10.1039/xxxxxxxxxx

Accurate Quantum Chemical Modelling of the Separation of Eu^{3+} from Am^{3+}/Cm^{3+} by Liquid-liquid Extraction with Cyanex272[†]

Xiaoyan Cao,[*a] Jun Zhang,[a] Daniel Weissmann[a], Michael Dolg[a] and Xuebo Chen[b]

Received Date
Accepted Date

DOI: 10.1039/xxxxxxxxxx

www.rsc.org/journalname

The experimentally observed extraction complexes of trivalent lanthanide Eu^{3+} and actinide Am^{3+}/Cm^{3+} cations with Cyanex272 [bis(2,4,4-trimethylpentyl) phosphinic acid, denoted as HC272] and Cyanex301 [bis(2,4,4-trimethylpentyl) dithiophosphinic acid, denoted as HC301] have been studied by using relativistic energy-consistent 4f- and 5f-in-core pseudopotentials for trivalent f elements, combined with density functional theory and a continuum solvation model. It has been found that, as a result of hydrogen bonding, HC272 exists primarily as a self-associated species, whereas HC301 is preferably a monomer. The calculations show that in case of all three M^{3+} (M=Eu, Am, Cm) ions for HC272 the extraction complexes M[H(C272)$_2$]$_3$ are formed prior to M(C272)$_3$, whereas for HC301 the extraction complexes M(C301)$_3$ have priority over M[H(C301)$_2$]$_3$. The calculated M-O and M-S bond lengths and the M-P distances of these prefered extraction complexes agree very well with the available experimental data. The obtained changes of the Gibbs free energies in the liquid-liquid extraction reactions (1): M^{3+}_{aqu} + 3(HC272)$_{2,org}$ → M[H(C272)$_2$]$_{3,org}$ + 3H$^{+}_{aqu}$ and (2): M^{3+}_{aqu} + 3HC301$_{org}$ → M(C301)$_{3,org}$ + 3H$^{+}_{aqu}$ agree with the experimentally observed thermodynamical priorities of HC272 and HC301, i.e., HC272 prefers Eu^{3+} over Am^{3+}/Cm^{3+} and HC301 prefers Am^{3+}/Cm^{3+} over Eu^{3+}. The obtained changes of the Gibbs free energies in reaction (2) (Eu, 68.1 kJ/mol; Am, 46.5 kJ/mol) agree quite well with the experimental findings (Eu, 63.3 kJ/mol; Am, 44.1 kJ/mol).

1 Introduction

Nuclear waste treatment is a well-known difficult problem affecting many countries worldwide. One important step of the extraction processes in nuclear waste management is to separate the minor and highly radiotoxic fission products of the neutron irradiation of U or Pu from the abundant and less harmful ones, e.g., the separation of so-called minor actinides such as Am^{3+} and Cm^{3+} from the light lanthanides[1,2]. Due to the very similar coordination chemistry of trivalent actinide (An^{3+}) and lanthanide (Ln^{3+}) cations the chemical separation of Ln^{3+} from An^{3+} is not easy. Chemical Ln^{3+}/An^{3+} separations usually exploit the different affinities of Ln^{3+} and An^{3+} ions to soft/hard Lewis base donor atoms in the interaction with the extractant, i.e., the affinity of An^{3+} to soft Lewis base donor atoms (e.g., S) is higher than the one of Ln^{3+}, whereas the affinity of Ln^{3+} to hard Lewis base donor atoms (e.g., O) is higher than the one of An^{3+}[3]. It was firstly reported by Zhu and coworkers[4] in 1995 that purified Cyanex301 [bis(2,4,4-trimethylpentyl)dithiophosphinic acid, denoted hereafter as HC301 and its anion as C301^{-}; cf. Fig. 1] in kerosene has a very high selectivity for Am^{3+}/Cm^{3+} over Eu^{3+}, when the ions are extracted from slightly acidic (pH ≈ 3-4) aqueous solution (Am/Eu separation factor > 5000). One year later the corresponding extraction enthalpies and entropies were determined experimentally, i.e., 18.10 kJ/mol and -87.10 J/(molK) for Am and 43.65 kJ/mol and -65.74 J/(molK) for Eu[5].

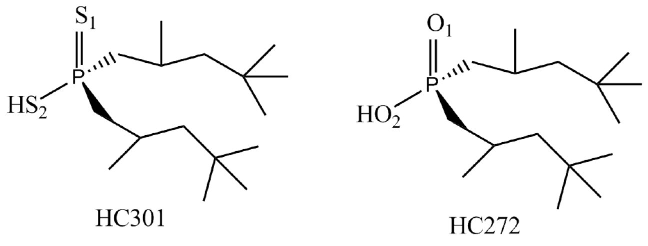

Fig. 1 Bis(2,4,4-trimethylpentyl)dithiophosphinic acid (HC301) and bis(2,4,4-trimethylpentyl)phosphinic acid (HC272)

Cyanex301 is a commercial extractant which is often used

---

[a] Theoretical Chemistry, University of Cologne, Greinstr. 4, 50939 Cologne, Germany. Fax: ++49 221 470 6896; Tel: ++49 221 470 6893; E-mail: x.cao@uni-koeln.de
[b] Department of Chemistry, Beijing Normal University, 100875 Beijing, P. R. China

[†] Electronic Supplementary Information (ESI) available: [details of any supplementary information available should be included here]. See DOI: 10.1039/b000000x/

for the separation of Co and Ni from other metals such as Mg and Mn, whereas the related Cyanex272 is industrially applied in large scales for the separation of Co from Ni. The extractant Cyanex272 was, e.g., also applied in the recycling of spent Li-ion and Ni-metal-hydride batteries (extracting Co, Ni and Cu)[6,7] or in the production of infrared-to-visible upconverting phosphor fine particles Y_2O_3:Yb,Er (extracting Y, Er and Yb)[8]. The chemically active component of Cyanex272 [bis(2,4,4-trimethylpentyl)phosphinic acid, denoted hereafter as HC272 and its anion as $C272^-$; cf. Fig. 1] is formally obtained by substituting O for S in HC301 and was reported to have a thermodynamical priority for Eu^{3+} over Am^{3+}/Cm^{3+}. By using Cyanex272 without purification, where a content of 85% of HC272 was assumed, Zhu and coworkers measured in 1996 an average separation factor for Eu/Am in n-heptane of about 11[5].

During the last two decades various experimental studies have been carried out to investigate the separation of Ln^{3+} and An^{3+} by using derivatives of bis(2,4,4-trimethylpentyl)phosphinic acid[9–12]. Jensen and Bond[10,11] have experimentally studied the liquid-liquid extraction of M^{3+} (M=Sm^{3+}, Nd^{3+}, Eu^{3+}, Am^{3+}, and Cm^{3+}) from the aqueous solution with purified Cyanex272 and Cyanex301 into the organic phase. The authors investigated especially the role of the aggregation of the extractant as well as the covalency in the metal-ligand interaction in the extraction complexes. The stoichiometries of these were found to be $M(C301)_3$ and $M[H(C272)_2]_3$, as verified by visible absorption spectroscopy and X-ray absorption fine structure (XAFS) measurements. Whereas in $M(C301)_3$ the three $C301^-$ ligands coordinate with two S donor atoms each in a roughly D_3 symmetric fashion to the metal center, it was found that three $[H(C272)_2]^-$ hydrogen-bonded dimers act as "bidentate" ligands in $M[H(C272)_2]_3$, with the O donor atoms forming a coordination octahedron (cf. Fig. 2). Jensen and Bond noticed that the metal-donor atom bond distances are indistinguishable within experimental error bars for trivalent lanthanide and actinide cations which are similar in size[10], i.e., the M-O/M-S bond lengths for $M[H(C272)_2]_3/M(C301)_3$ with M=Cm, Nd, and Sm are 2.32 ± 0.01/2.826 ± 0.008, 2.345 ± 0.004/2.852 ± 0.007, and 2.301 ± 0.003/2.803 ± 0.006 Å, respectively. Thus, despite the pronounced selectivity of HC301 for actinide(III) ions a possible underlying enhanced covalency in the An-S bonds does not manifest itself structurally in shorter bond distances relative to Ln-S bonds.

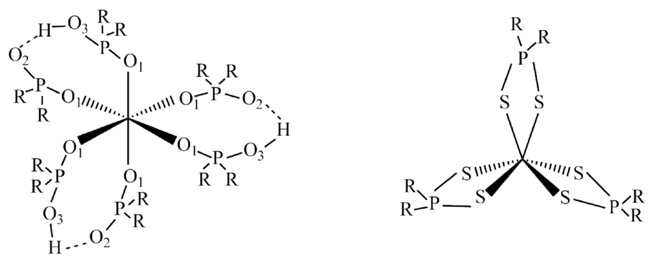

Fig. 2 Structures of the complexes of trivalent Eu, Am, and Cm with HC272 and HC301. R=2,4,4-trimethylpentyl

Quantum chemical investigations of the extraction complexes can help to determine reasons of the preference of an extractant for a specific ion and possibly also assist in the construction of more efficient extractants once the reliability of the chosen computational model is established. However, the extremely complex electronic structure of most f elements, which contains numerous low-lying electronic states and exhibits large relativistic effects as well as strong electron correlation contributions, poses considerable difficulties to theoretical work. Among the approaches developed in relativistic quantum chemistry, the method of ab initio pseudopotentials (PPs) is one of the most successful ones.[13] Because of the core-valence separation, only the chemically relevant valence electron system is treated explicitly and relativistic effects are only implicitly accounted for by a proper adjustment of free parameters in the valence-only Hamiltonian. Whereas the first aspect leads to a reduction of the computational effort, the second allows an inclusion of the scalar-relativistic contributions in a nonrelativistic framework. For f elements, relativistic energy-consistent ab initio 4f-in-core[14,15] and 4f-in-valence[16] PPs were first published in 1989 for lanthanides, and corresponding 5f-in-valence PPs[17] for actinides were derived in 1994. 5f-in-core[18,19] actinide PPs became available in 2007, and many applications have shown that they are useful and reliable[13,20,21].

In a previous publication we reported structural and energetic data for the separation of Am^{3+}/Cm^{3+} from Eu^{3+} by liquid-liquid extraction with HC301[20] obtained from quantum chemical calculations using energy-consistent 4f-[14,15,22] and 5f-[19] in-core pseudopotentials for trivalent f elements, a continuum solvation model and density functional theory (DFT) as well as second-order Møller-Plesset perturbation theory (MP2). The obtained changes of Gibbs free energies in the extraction reactions agree with the thermodynamical priority for Am^{3+} and Cm^{3+}. Moreover, the hydration Gibbs free energies for M^{3+} (M=Eu, Am, Cm) were found to play an important role for the high selectivity of HC301 for Am^{3+} and Cm^{3+} over Eu^{3+}.[20] The role of covalency in the metal-ligand interactions and the reliability of f-in-core PPs to produce correct trends in the corresponding bond distances at the DFT level was also discussed[21]. It is important to notice that f-in-valence PPs as well as all-electron (AE) approaches in combination with standard DFT parametrizations have difficulties to treat accurately the Eu^{3+} ion and due to an erroneous overfilling of the $4f^6$ subshell yield too long Eu-ligand bond distances for soft donors[21,23]. Thus, although the f-in-core PP approach uses the drastic approximation to eliminate the (partially occupied) f shell from the explicit quantum chemical treatment, it does not necessarily yield worse results than standard treatments. Note that by means of construction of the f projectors a partial charge transfer from the ligand donor atoms to the f shell of the metal center is still possible[15,19].

The computational modeling and simulations of Ln^{3+}/An^{3+} separation processes were recently reviewed by Lan et al.[24]. To our knowledge, so far there is no theoretical work published on the complexation of Ln^{3+} and An^{3+} ions with HC272. Therefore the present work examines the extraction reactions of Eu^{3+}, Am^{3+} and Cm^{3+} with HC272 using f-in-core PPs at the DFT level. Solvent effects are taken into account by using the COSMO (conductor-like screening model) approach[25]. The structures and stabilities of the extractants and extraction complexes, as well as the changes of the Gibbs free energy for the complexation in gas phase and aqueous solution are discussed. The corresponding Gibbs free energy changes for the extraction from the aqueous phase with n-heptane for HC272 and kerosene for HC301 are evaluated on the basis of simple assumptions concerning the distribution of the involved ions/molecules between the aqueous and organic phase. Our previous work demonstrated that the computational protocol applied here is able to correctly predict the selective priority of HC301 for Am^{3+} over Eu^{3+}.[20] The present work aims to demonstrate that this approach is able to yield for the same ions a reverse order of extraction preference when the extractant is modified, i.e., it yields a selective priority of HC272 for Eu^{3+} over Am^{3+}. The agreement of the computational results with experimental evidence supports the usefulness of the model to study theoretically related liquid-liquid separations and possibly also to predict the outcome for different ions and extractants.

2 Computational Methods

The method of relativistic energy-consistent ab initio pseudopotentials (PPs) is described in detail elsewhere[13] and will be outlined here only briefly. The valence-only model Hamiltonian for a system with n valence electrons and N nuclei with charges Q is given as

$$H_v = -\frac{1}{2}\sum_i^n \Delta_i + \sum_{i<j}^n \frac{1}{r_{ij}} + V_{av} + \sum_{I<J}^N \frac{Q_I Q_J}{r_{IJ}} \qquad (1)$$

Here i and j are electron indices and I, J are nuclear indices. In the usual approximation the molecular PP V_{av} is a superposition of atom-centered PPs

$$V_{av} = \sum_I^N V_{av}^I \qquad (2)$$

V_{av}^I denotes a spin-orbit averaged relativistic PP in a semilocal form for a core I with charge Q_I

$$V_{av}^I = -\sum_i^n \frac{Q_I}{r_{iI}} + \sum_i^n \sum_{l,k} A_{lk}^I exp(-a_{lk}^I r_{iI}^2) P_l^I \qquad (3)$$

P_l^I is the projection operator onto the Hilbert subspace of angular momentum l with respect to center I. The free parameters A_{lk}^I and a_{lk}^I are adjusted to reproduce the total valence energies of a multitude of low-lying electronic states of the neutral atom I and its ions. Large-core PPs for lanthanides[14,15,22]/actinides[19] have been used, i.e., the 1s-4f/1s-5f shells were included in the PP core, while all others with main quantum number larger than 4/5 were treated explicitly (11 valence electrons for Eu, Am, Cm). The reference data used to determine V_{av} has been taken from all-electron (AE) calculations using the so-called Wood-Boring (WB) scalar-relativistic Hartree-Fock (HF) approach. Both AE WB and PP calculations have been performed with an atomic finite-difference HF scheme in order to avoid basis set effects in the determination of the PP parameters.

Energy-consistent scalar-relativistic WB-adjusted 52-, 84-, and 85-electron core PPs were selected for Eu, Am and Cm, respectively. The corresponding basis sets were taken from the basis set library of the TURBOMOLE program package[26], i.e., ECP52MWB-I for Eu, ECP84MWB-AVDZ for Am and ECP85MWB-AVDZ for Cm. These sets correspond to (7s6p5d)/[6s5p4d][14,22] for Eu, and to (7s6p5d)/[4s3p3d][19] for Am and Cm. Since only extraction and hydration complexes of M^{3+} ions (M = Eu, Am, Cm) are considered, where the valence d shell is not occupied, these sets already allow for a polarization of the central ions. All other lighter atoms were treated at the AE level, and the standard def-SV(P) basis sets were used, i.e., H(4s)/[2s][27], C, O (7s4p1d)/[3s2p1d][28], and P, S (10s7p1d)/[4s3p1d][28] (denoted hereafter as basis set A). In order to check for possible basis set deficiencies larger basis sets were applied too, i.e., a (8s7p6d3f2g)/[6s5p5d3f2g] basis set for Eu[14,22,29] and (7s6p5d2f)/[5s4p4d2f] basis sets for Am and Cm[19], which are named Eu ECP52MWB-II, Am ECP84MWB-AVTZ, and Cm ECP85MWB-AVTZ in the TURBOMOLE program package[26]. For the lighter elements def2-TZVP basis sets were selected, i.e., H (5s1p)/[3s1p][27], C, O (11s6p2d1f)/[5s3p2d1f][30], and P, S (14s9p3d1f)/[5s5p2d1f][31] (denoted as basis set B hereafter). Moreover the optimized auxiliary def2-TZVP basis sets, i.e., H (4s3p2d) / [4s2p1d][30], C, O (8s6p5d3f1g) / [8s6p4d3f1g][30], and P, S (10s7p7d5f2g)/[9s7p6d5f2g][32] have been applied in the calculations using the resolution of the identity second-order Møller-Plesset perturbation theory approach (RIMP2).[33]

Most of the calculations have been carried out at the DFT level with the TURBOMOLE program package.[26] The generalized gradient approximation (GGA) type density functional BP86 was applied, i.e., the Hartree-Fock exchange energy is approximated by using the gradient-corrected exchange-energy functional proposed by Becke[34] in 1988 and the electron correlation energy is approximated by using the density functional proposed by Perdew[35] in 1986. Calculations taking into account hydration effects were carried out using COSMO[25], where the dielectric constant for water was used, $\varepsilon = 80$. Solvation effects for kerosene, n-heptane and benzene were calculated correspondingly using $\varepsilon = 1,80$, 1.92 and 2.27, respectively. COSMO is a variant of continuum solvation models which uses a scaled conductor boundary condition for the calculation of the polarization charges of a molecule (solute) in a continuum (solvent). For the cavity generation, the previously used atomic radii (Å)[20] were taken in our COSMO calculations: C 1.989; H 1.404; O 1.7784; S 2.106; P 2.106; Eu 1.820; Am 2.045; Cm 2.020. Additional geometry optimizations were performed using the resolution of the identity second-order Møller-Plesset perturbation theory approach (RIMP2) implemented in TURBOMOLE. For calibrating the electronic energy contributions derived at the DFT level single-point incremental coupled cluster (CC) calculations using the MOLPRO program package[36] for CCSD(T) calculations and an in-house C++ code for the incremental scheme[37–39] were carried out. MOLPRO was also applied for the energy decomposition analysis.

2.1 Extractant Oligomerization

The structures of the extractants, i.e, HC272, HC301, $[HC272]_2$, $[HC301]_2$, have been fully optimized by using basis sets A and B at the DFT/BP86 level, as well as at the RIMP2 level by using the larger basis set B. Due to the limit of our computational resources vibrational analyses have been only done at the DFT level. For model structures of oligomers of the extractants, i.e., $[HX_2P(CH_3)_2]_n$ (X=O, S; n=1-4), based on the optimized geometries at the DFT/BP86 level using basis set B, single-point coupled cluster (CC) calculations using correlation-consistent basis sets of polarized valence triple-zeta quality[40] within a variant of the so-called incremental scheme (inc3-db-B0, third-order incremental scheme with dual basis set and zero-buffer approach)[37–39] have also been carried out.

The change of the Gibbs free energy in the gas phase (ΔG_g) as well as for an organic phase (ΔG_{org}) has been calculated for the dimerization reaction

$$2\ (\mathrm{HY}) \xrightarrow{\Delta G_g,\Delta G_{org}} [\mathrm{HY}]_2 \qquad (4)$$

where Y=C272 and C301. The subscript "org" indicates benzene or n-heptane as the solvent. In order to study higher aggregation of the extractants we also considered with extractant models $HX_2P(CH_3)_2$ (X=O, S) the oligomerization reactions

$$\mathrm{I:}\ n[\mathrm{HX_2P(CH_3)_2}] \xrightarrow{\Delta G_g,\Delta G_{org}} [\mathrm{HX_2P(CH_3)_2}]_n \qquad (5)$$

for $n = 2,3,4$,

$$\mathrm{II:}\ [\mathrm{HX_2P(CH_3)_2}]_n + \mathrm{HX_2P(CH_3)_2} \xrightarrow{\Delta G_g,\Delta G_{org}} [\mathrm{HX_2P(CH_3)_2}]_{n+1} \qquad (6)$$

for $n = 2,3$, and

$$\mathrm{III:}\ 2[\mathrm{HX_2P(CH_3)_2}]_2 \xrightarrow{\Delta G_g,\Delta G_{org}} [\mathrm{HX_2P(CH_3)_2}]_4 \qquad (7)$$

Here benzene was assumed as a solvent. The ΔG_{org} may be obtained by the change of the gas-phase Gibbs free energies, ΔG_g, by adding corrections $\Delta\Delta G_{org}$ for solvent effects:

$$\Delta G_{org} = \Delta G_g + \Delta\Delta G_{org} \qquad (8)$$

The gas-phase Gibbs free energy for all reactants and products in the reactions listed above, i.e., $G_g([HY]_n)$ (n=1, 2, 3; Y=C272, C301) and $G_g([HX_2P(CH_3)_2]_n)$ (n=1, 2, 3, 4; X=O, S), were determined from the gas-phase total energy by adding the zero-point energy and a thermal correction by using the ideal gas model for T= 298.15 K and p=0.1 MPa. The corrections for solvent effects $\Delta\Delta G_{org}$ for the monomers HC272 and HC301, as well as for model oligomers $[HX_2P(CH_3)_2]_n$ (n=1, 2, 3, 4; X=O, S), were approximated by single-point energy calculations for fixed gas-phase molecular structures by addressing bulk solvation effects with the COSMO (conductor-like screening model) approach[25].

2.2 Liquid-liquid Extraction

The structures of the experimentally observed extraction complexes $M[H(C272)_2]_3$ of M^{3+} (M=Eu, Am, Cm) with HC272 have been fully optimized by using basis sets A and B at the DFT BP86 level. Due to the limit of our computational resources it was impossible to carry out the vibrational analyses with basis set B for the extraction complexes $M[H(C272)_2]_3$ (322 atoms). Therefore, for the calculations of these contributions to the Gibbs free energies of the extraction processes basis set A was chosen. As judged from the results of our previous study of the $M(C301)_3$ extraction complexes the usage of basis set A instead of B for the vibrational contributions leads to a shift of the final ΔG_s and ΔG_e values, but not to a reversal of trends for the three metal ions Eu^{3+}, Am^{3+}, and Cm^{3+}[20].

The change of the Gibbs free energy, ΔG_e, of the following extraction equation has been calculated

$$\mathrm{M}^{3+}_{aqu} + 3(\mathrm{HC272})_{2,org} \xrightarrow{\Delta G_e} \mathrm{M[H(C272)_2]}_{3,org} + 3\mathrm{H}^+_{aqu} \qquad (9)$$

In 9, the initial state supposes a metal ion in aqueous phase, with HC272 residing in the organic (n-heptane) phase, whereas in the final state, the ion is complexed by three $H(C272)_2^-$ anions in the organic phase after release of three protons, which remain in the aqueous phase. The change of the Gibbs free energies in aqueous solution, ΔG_s, and for the extraction, ΔG_e, may be obtained by the change of the gas-phase Gibbs free energies , ΔG_g, by adding corrections $\Delta\Delta G_s$ and $\Delta\Delta G_e$, respectively, for solvent effects:

$$\Delta G_{s,e} = \Delta G_g + \Delta\Delta G_{s,e} \qquad (10)$$

where

$$\begin{aligned}\Delta G_g &= G_g(\mathrm{M[H(C272)_2]_3}) + 3G_g(\mathrm{H^+}) \\ &\quad - G_g(\mathrm{M^{3+}}) - 3G_g([\mathrm{HC272}]_2) \\ \Delta\Delta G_{s,e} &= \Delta G_{sol}(\mathrm{M[H(C272)_2]_3}) + 3\Delta G_{sol}(\mathrm{H^+}) \\ &\quad - \Delta G_{sol}(\mathrm{M^{3+}}) - 3\Delta G_{sol}([\mathrm{HC272}]_2) \qquad (11)\end{aligned}$$

Here the subscript "sol" indicates water (aqu) and/or n-heptane (org) as the solvent. The gas-phase Gibbs free energies for $M[H(C272)_2]_3$, H^+, $(HC272)_2$, and M^{3+}, i.e., $G_g([MH(C272)_2]_3)$, $G_g(H^+)$, $G_g([HC272]_2)$, and $G_g(M^{3+})$, were determined from the gas-phase total energy by adding the zero-point energy and a thermal correction by using the ideal gas model for T= 298.15 K and p=0.1 MPa. The hydration Gibbs free energies for $M[H(C272)_2]_3$ and $[HC272]_2$, i.e., $\Delta G_{org}(M[H(C272)_2]_3)$ and $\Delta G_{org}([HC272]_2)$, were determined by single-point energy calculations for fixed gas-phase molecular structures and subsequent COSMO (conductor-like screening model)[25] calculations to account for bulk solvation effects. Whereas for $\Delta G_{aqu}(H^+)$ and $\Delta G_{aqu}(Eu^{3+})$ experimental data exists (H^+ -1104.5 kJ/mol[41], Eu^{3+} -3364.1 kJ/mol),[42] this does not seem to be the case for $\Delta G_{aqu}(Am^{3+})$ and $\Delta G_{aqu}(Cm^{3+})$. In order to be able to compare the complex formation and extraction for Eu^{3+} with Am^{3+} and Cm^{3+} we rely on the published results (Eu^{3+} -3308 kJ/mol[43], Am^{3+} -3207 kJ/mol[44], Cm^{3+} -3235 kJ/mol[44]) obtained at the MP2 level for coordination number 9 and derived from a cluster cycle as well as on semiempirical data (Eu^{3+} -3252 kJ/mol[45], Am^{3+} -3159 kJ/mol[46], Cm^{3+} -3225 kJ/mol[46]). Based on the M[H(C272)$_2$]$_3$ geometry data and the calculated ΔG_s values the selectivity of Cyanex272 for Ln^{3+} over An^{3+} will be discussed. We note that the value for $\Delta G_{aqu}(H^+)$ of Tissandier et al.[41] used here was critically analyzed for correctness and recommended by Camaioni and Schwerdtfeger[47] for further applications. This value was also confirmed by Truhlar and coworkers within 0.8 kJ/mol for a larger reference data set[48].

3 Results and Discussion

3.1 Structures of extractants HC272 and HC301

In 1995 Sole and Hiskey[49] studied the degrees of aggregation of the extractants HC272 and HC301 in benzene as solvent using molar mass determinations by means of vapor pressure osmometry (VPO). They found that HC272 exists predominantly as a dimer, whereas HC301 exists as monomer. Grigorieva and coworkers[50] observed that HC301 in organic solvents such as nonane is not only present as a monomer, but also forms dimers (HC301)$_2$ and tetramers (HC301)$_4$ via S-H-S hydrogen bonds. To the best of our knowledge there is no theoretical work on the degrees of aggregation of HC272 and HC301 so far.

Since the aggregation might have noticeable effects on the energetics of the extraction, we investigated this issue further. We have optimized the geometries of the monomers and dimers of HC272 and HC301 at the DFT/BP86 and RIMP2 level. The most important geometrical parameters of the optimized structures for HC272, [HC272]$_2$, HC301, and [HC301]$_2$ have been compiled in Tab. 1 and 2. The changes of the Gibbs free energy in the gas phase ΔG_g (kJ/mol) as well as in the organic phase ΔG_{org} (kJ/mol) have been calculated for the dimerization of HC272 and HC301 (see reaction eqn. 4), cf. Tab. 3. For convenience of the discussion the gas-phase Gibbs free energy change ΔG_g is split into the electronic contribution and the one arising from vibration, rotation and translation:

$$\Delta G_g = \Delta G_g^{elec} + \Delta G_g^{vib+rot+trans} \tag{12}$$

Let us first check the performance of the applied basis sets. Two basis sets were used for geometry optimizations, i.e., basis set A, def-SV(P) and basis set B, def2-TZVP for C, H, O, S and P, respectively. For [HC272]$_2$ and [HC301]$_2$ the application of both basis sets showed that a hydrogen bond is formed, cf. Fig. 3. The obtained bond lengths for basis set A/B at the DFT/BP86 level are $R(O_1-H) = 1.412/1.469$ Å for [HC272]$_2$ and $R(S_1-H)$ 2.194/2.256 Å for [HC301]$_2$, respectively. When using the larger basis set B the hydrogen bonds, O$_1$-H and S$_1$-H, get by 0.057 Å and 0.068 Å longer, respectively, whereas the other bonds get slightly shorter compared to results obtained with basis set A. For HC272 and [HC272]$_2$ the average differences are 0.014, 0.024, 0.026, and 0.02 Å for the P-C, P=O$_1$, P-O$_2$, and O$_2$-H bonds, respectively; for HC301 and [HC301]$_2$ the average differences are 0.014, 0.017, 0.024, and 0.016 Å for the P-C, P=S$_1$, P-S$_2$, and S$_2$-H bonds, respectively. Bond angles are even less affected by the application of different basis sets, i.e., the differences for the bond angles are at most 1°. Comparing to the results obtained at the DFT/BP86 level the optimized bond lengths at the MP2 level for HC272 monomer and HC272 dimer are on average 0.023, 0.013, 0.015, and 0.025 Å shorter for P-C, P=O$_1$, P-O$_2$, and O$_2$-H bonds, respectively. For the monomer and dimer of HC301 the optimized bond lengths for P-C, P=S$_1$, P-S$_2$, and S$_2$-H bonds at the MP2 level are 0.027, 0.022, 0.029, and 0.021 Å shorter, respectively. However for the hydrogen bonds in the dimers, i.e., O$_1$-H and S$_1$-H, the calculated bond lengths at the MP2 level are 0.096 and 0.106 Å longer comparing to results obtained at the DFT/BP86 level.

	HC272			[HC272]$_2$		
	SV(P)^b	def2-TZVP^c		SV(P)^b	def2-TZVP^c	
	BP86	BP86	RIMP2^d	BP86	BP86	RIMP2^d
R(P-C)	1.841	1.827	1.803	1.838	1.824	1.802
R(P=O$_1$)	1.515	1.494	1.484	1.548	1.521	1.506
R(P-O$_2$)	1.674	1.644	1.626	1.605	1.583	1.580
R(O$_2$-H)	0.984	0.975	0.970	1.085	1.054	1.018
R(O$_1$-H)^a				1.412	1.469	1.565
∠ O$_1$PO$_2$	112	112	112	114.8	114.6	114.6
∠ CPC	106	105	106	108.9	108.0	107.6

Table 1 Calculated averaged bond lengths (Å), averaged bond angles (deg) for HC272 and [HC272]$_2$

^{a}: For HC272 dimer a hydrogen bond is formed between one O$_1$ atom of one HC272 and the hydrogen atom of another HC272. cf. Fig. 3 ^{b}: basis set A, i.e., O (7s4p1d)/[3s2p1d][28], C (7s4p1d)/[3s2p1d][28], H(4s)/[2s][27], S (10s7p1d)/[4s3p1d][28], and P (10s7p1d)/[4s3p1d][28]; ^{c}: basis set B, i.e., O(11s6p2d1f)/[5s3p2d1f], C (11s6p2d1f)/[5s3p2d1f][30], H (5s1p)/[3s1p][27], and P (14s9p3d1f)/ [5s5p2d1f][30] ^{d}: ri basis set, i.e., C (8s6p5d3f1g) / [8s6p4d3f1g][30], H (4s3p2d) / [4s2p1d], O (8s6p5d3f1g) / [8s6p4d3f1g][30], P (10s7p7d5f2g)/[9s7p6d5f2g][32]

	HC301			[HC301]$_2$		
	SV(P)^b	def2-TZVP^c		SV(P)^b	def2-TZVP^c	
	BP86	BP86	RIMP2^d	BP86	BP86	RIMP2^d
R(P-C)	1.864	1.850	1.822	1.857	1.843	1.817
R(P=S$_1$)	1.966	1.952	1.933	2.001	1.981	1.956
R(P-S$_2$)	2.190	2.159	2.122	2.132	2.115	2.094
R(S$_2$-H)	1.368	1.352	1.340	1.417	1.393	1.362
R(S$_1$-H)^a				2.194	2.256	2.362
∠ S$_1$PS$_2$	113.9	113.8	113.2	116.0	115.7	115.5
∠ CPC	102.0	101.5	102.5	107.5	107.1	106.6

Table 2 DFT/BP86 calculated averaged bond lengths (Å), averaged bond angles (deg) for HC301 and [HC301]$_2$

^{a}: For HC301 dimer the S$_1$ atom of one HC301 forms a hydrogen bond with the H atom of another HC301. ^{b}: basis set A, i.e., S (10s7p1d)/[4s3p1d][28], C,H,P cf. Tab. 1; ^{c}: basis set B, i.e., S (14s9p3d1f)/[5s5p2d1f][31], C,H,P cf. Tab. 1 ^{d}: ri basis set, i.e., S (10s7p7d5f2g)/[9s7p6d5f2g][32], C,H,P; cf. Tab. 1

Considering only the electronic energy contributions both dimers [HC272]$_2$ and [HC301]$_2$ are more stable than the corresponding monomer pairs 2[HC272] and 2[HC301], respectively. Taking into account also the contributions of vibration, rotation and translation it has been found that in the gas phase the dimer [HC272]$_2$ is more stable than two HC272 monomers, whereas in contrast to this two HC301 monomers were found to be more stable than the [HC301]$_2$ dimer, cf. Tab. 3. At the DFT/BP86 level the obtained Gibbs free energy changes in the dimerization reaction 2[HC272] → [HC272]$_2$ are -62.2 and -38.6 kJ/mol for basis set A and B, respectively, whereas the corresponding results for the reaction 2[HC301] → [HC301]$_2$ are 25.6 and 42.5 kJ/mol, respectively. When estimating the basis set superposition error by using the Boys-Bernardi counterpoise scheme[51] (the monomer calculations were performed at their geometries in the dimers) the differences between the results for the two basis sets become

	ΔG_g		$\Delta\Delta G_{org}$		ΔG_{org}	
	ΔG_g^{elec} A/B	$\Delta G_g^{vib+rot+trans}$ A/B	^{b} A/B	^{c} A/B	^{b} A/B	^{c} A/B
HC272						
DFT/BP86	-98.8/-74.4	36.6/35.8	7.6/13.1	9.3/16.0	-54.6/-25.5	-52.9/-22.6
DFT/BP86+CPC	-57.4/-69.4				-13.2/-20.5	-11.5/-17.6
RIMP2	/-99.2		/12.7	/15.5	/-50.9	/-48.1
RIMP2+CPC	/-82.8				/-34.5	/-31.7
HC301						
DFT/BP86	-18.7/-10.2	44.3/52.7	2.3/5.6	2.8/6.9	27.9/48.1	28.4/49.4
DFT/BP86+CPC	1.8/ -6.9				48.4/51.4	48.9/52.7
RIMP2	/-53.4		/5.0	/6.1	/ 4.3	/5.4
RIMP2+CPC	/-39.9				/17.8	/18.9

Table 3 Calculated change in the Gibbs free energy contribution ΔG_g and ΔG_{org} (kJ/mol), in the HC272 and HC301 dimerization 2HL → $[HL]_2$, L=C272, C301[a]

[a] $\Delta G_{org}=\Delta G_g+\Delta\Delta G'_{org}$. .../... refers to the results obtained with basis sets A/B (cf. Tab. 1). For the RIMP2 calculations only basis sets B were used and $\Delta G_g^{vib+rot+trans}$ was taken from the DFT/BP86 results. CPC denotes counterpoise-corrected results. [b]: n-heptane (dielectric constants: 1.92 (org)). [c]: benzene (dielectric constants: 2.27 (org).

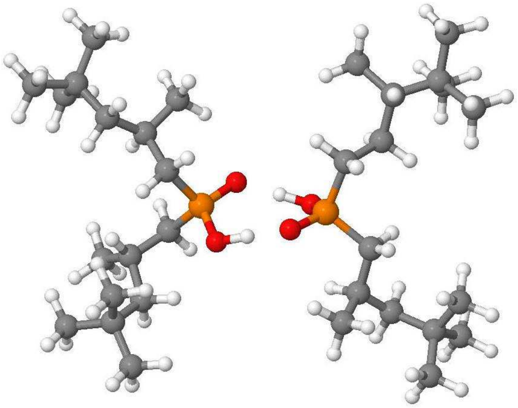

Fig. 3 Calculated structure of the HC272 dimer

significantly smaller. The dimerization energies for basis set A and B, respectively, are now -20.8 and -33.6 kJ/mol for HC272 as well as 46.1 and 45.8 kJ/mol for HC301. We attribute the different tendencies to form dimers to the stronger intramolecular hydrogen bonds in $[HC272]_2$ compared to $[HC301]_2$.

By using the COSMO approach we calculated the Gibbs free energy changes ΔG_{org} for the dimerization reactions eqn. 4 of HC272 and HC301 in the solvents n-heptane and benzene, respectively, cf. Tab. 3. For HC272 comparing to ΔG_g the ΔG_{org} values are increased for basis set A/B by about 7/13 kJ/mol for n-heptane and by 9/16 kJ/mol for benzene. For HC301 the effect of the solvent is smaller comparing to HC272, i.e., ΔG_{org} is increased for basis set A/B by about 2/5 kJ/mol for n-heptane and by 3/7 kJ/mol for benzene.

Compared to the counterpoise-corrected DFT/BP86 results obtained with basis set B for ΔG_g^{elec} the corresponding MP2 values are about 13 and 33 kJ/mol lower for the HC272 and HC301 dimerizations, respectively. Due to the limit of our computational resources we were unable to do the vibrational analyses for the dimers of HC272 and HC301 at the MP2 level. For the monomers of HC272 and HC301 it has been found that the obtained $G_g^{vib+rot+trans}$ values at the MP2 level are only 14 and 8 kJ/mol smaller than results calculated at the DFT/BP86 level using basis sets B. Therefore we took the calculated $\Delta G_g^{vib+rot+trans}$ with basis sets B at the DFT/BP86 level and estimated the ΔG_{org} at the MP2 level. The corresponding results (-31.7 kJ/mol for HC272 and 18.9 kJ/mol for HC301, cf. Tab. 3) in the solvent benzene agree reasonably well with the values obtained at the DFT/BP86 level (-17.6 kJ/mol for HC272 and 52.7 kJ/mol for HC301), i.e, HC272 forms dimers, whereas HC301 is preferably monomeric.

Model systems, i.e., the rest group 2,4,4-trimethylpentyl for HC272 and HC301 is replaced by methyl, $[HX_2P(CH_3)_2]_n$ (X=O, S; n=1, 2, 3, 4) have been calculated to estimate the stability of trimers and tetramers. The obtained Gibbs free energy changes in gas phase ΔG_g as well as in the organic phase ΔG_{org} (solvent: benzene) for the reactions I, II and II are shown in Tab. 4 and 5.

In analogy to the real system all calculations have shown that the dimer containing oxygen, i.e., $[HO_2P(CH_3)_2]_2$, is more stable than two monomers $HO_2P(CH_3)_2$, whereas the dimer containing sulfur, i.e., $[HS_2P(CH_3)_2]_2$, is less stable than two monomers $HS_2P(CH_3)_2$, cf. Tab. 4. At the DFT/BP86 level the reaction $2HO_2P(CH_3)_2 \rightarrow [HO_2P(CH_3)_2]_2$ is clearly exergonic, i.e., the calculated changes of the Gibbs free energies ΔG_g and ΔG_{org} are -51.9 and -32.6 kJ/mol, respectively. For the endergonic reaction $2HS_2P(CH_3)_2 \rightarrow [HS_2P(CH_3)_2]_2$ the corresponding ΔG_g and ΔG_{org} values are 19.7 and 28.6 kJ/mol, respectively. The ΔG_{org} values for the trimerization and tetramerization reactions of $HO_2P(CH_3)_2$ are both close to zero, i.e., -3.9 and 3.1 kJ/mol, whereas it is 31.8 kJ/mol for the formation of the tetramer from two dimers, cf. Tab. 4 and 5. This implies that the dimer of the extractant HC272 is the dominating form, whereas the monomer as well as higher aggregates may be present to a lesser extent. In contrast to this the extractant HC301 most likely exists mainly as a monomer since the calculated ΔG_{org} values for the corresponding oligomerization reactions are all positive, cf. Tab. 4 and 5.

In order to check the results of the DFT/BP86 calculations we performed single-point CC calculations using correlation-consistent basis sets of polarized valence triple-zeta quality[40] by using the incremental scheme in the variant developed by Zhang and Dolg[37–39]. The corresponding results for geometries optimized with basis sets B are shown in Tab. 4 and 5. Comparing

	$[HX_2P_2(CH_3)_2]_2$		$[HX_2P_2(CH_3)_2]_3$			
	X=O	X=S	X=O		X=S	
	I	II	I	II	I	II
DFT BP86[b]	-51.9/-32.6	19.7/28.6	-69.6/-36.4	-17.7/-3.9	55.4/70.8	35.7/42.3
inc3-CCSD(T)[c]	-63.0/-43.7	4.4/13.2	-100.4/-67.3	-37.5/-23.6	24.1/39.5	19.7/26.3
inc3-CCSD[c]	-56.7/-37.3	13.8/22.6	-89.0/-55.8	-32.3/-18.4	40.5/55.9	26.7/33.3

Table 4 Calculated change of the Gibbs free energy in the gas phase ΔG_g and in the organic phase (solvent: benzene) ΔG_{org} (kJ/mol) in the reactions 5 and 6[a]

[a] .../... refers to the results $\Delta G_g/\Delta G_{org}$, dielectric constant of benzene: 2.27. The solvent contribution to the change of the Gibbs free energy in the reactions was obtained from the calculated energy difference at the DFT/BP86 level using basis set B (cf. Tab. 1) between the energy obtained in the gas phase and the energy obtained in the organic phase by using the COSMO model, cf. text. [b] geometry optimized by using basis set B, cf. Tab. 1; [c] single-point CCSD(T) and CCSD calculations within the incremental scheme[37,38] using basis set cc-pVTZ[40] for the geometry optimized at the DFT/BP86 [a] level.

	X=O		
	I	II	III
DFT BP86[b]	-81.2/-33.3	-11.6/3.1	22.6/31.8
inc3-CCSD(T)[c]	-127.9/-80.1	-27.5/-12.8	-2.0/7.2
inc3-CCSD[c]	-112.6/-64.8	-23.6/-9.00	0.7/9.9
	X=S		
	I	II	III
DFT BP86[b]	85.3/107.5	29.9/36.7	45.8/50.4
inc3-CCSD(T)[c]	28.4/50.5	4.2/11.0	19.6/24.1
inc3-CCSD[c]	50.2/72.4	9.8/16.5	22.6/27.3

Table 5 Calculated change of the Gibbs free energy in the gas phase ΔG_g and in the organic phase (solvent: benzene) ΔG_{org} (kJ/mol) in the reactions 5, 6, and 7 for the product of $[HX_2P_2(CH_3)_2]_4$ (X= O, S)[a]. explanations [a], [b], [c], cf. Tab. 4

	Eu	Am	Cm
$R(M\text{-}O_1)$	2.340/2.337	2.397/2.403	2.381/2.386(2.32±0.01[10])
R(M-P)	3.793/3.776	3.841/3.835	3.826/3.817
$R(O_1\text{-}P)$	1.559/1.535	1.559/1.535	1.559/1.535
$R(O_2\text{-}P)$	1.568/1.540	1.569/1.541	1.569/1.542
$R(O_3\text{-}P)$	1.586/1.560	1.586/1.559	1.586/1.558
$R(O_2\text{-}H)$	1.283/1.295	1.282/1.289	1.281/1.282
$R(O_3\text{-}H)$	1.160/1.138	1.162/1.143	1.162/1.147
$\angle O_1MO_1$	90.0/90.1	90.0/90.1	90.0/90.0
$\angle O_1PO_2$	114.8/115.1	114.9/115.1	114.9/115.1
$\angle O_1O_1O_1M$	2.2/2.5	2.1/2.7	2.0/2.4

Table 6 Selected averaged bond lengths (Å) and averaged bond angles (deg) for $M[H(C272)_2]_3$ (M= Eu, Am, Cm, HL= Cyanex 272) calculated at DFT/BP86 level [a] in comparison to available experimental data (in parentheses)

[a] .../... refers to the results obtained with basis sets A/B (cf. Tab. 1). $O_i (i = 1, 2, 3)$ refers to oxygen bound to different atoms, cf. Fig. 2.

to the DFT/BP86 results the ab initio values for ΔG_{org} are systematically smaller, but the general trend obtained at the DFT/BP86 level is not changed. In case of the HC301 model systems the formation of oligomers is still unlikely, whereas for the HC272 model systems the formation of trimers and tetramers becomes more favored, i.e., for the HC301 model the values $\Delta G_{org}/n$ are 6.6, 13.2 and 12.6 kJ/mol for $n = 2$, 3, and 4, respectively, whereas for the HC272 model values of -21.9, -22.4 and -20.0 kJ/mol are obtained. Based on the above calculations we conclude that HC272 exists primarily as self-associated species whereas HC301 exists as a monomer.

3.2 Structures of Extraction Complexes $M[H(C272)_2]_3$ (M=Eu, Am, Cm)

The most important geometrical parameters of the optimized structures by using basis sets A and B, as well as available experimental data[10], are listed in Tab. 6. Additional information is provided in the supplementary material. Vibrational analyses were only done for basis set A due to the limit of our computational resources. It has been shown that the six oxygen atoms (O_1 in Fig. 2) surrounding the central metal ion M^{3+} (M=Eu, Cm, Am) have nearly octahedral symmetry, i.e., for $M[H(C272)_2]_3$ by using basis set B the calculated mean absolute deviation of the bond lengths $R(O_1\text{-}M)$ from the average value is about 0.01 Å; the deviation of $\angle O_1MO_1$ comparing to the ideal 90° is less than 3°; the dihedral angles between three O_1 atoms and M are about 2°, cf. Tab. 6. Comparing to basis set A the application of basis set B increases slightly the bond lengths of $Am\text{-}O_1$ and $Cm\text{-}O_1$ by 0.006 and 0.005 Å, respectively, but the bond length of $Eu\text{-}O_1$ is decreased slightly by 0.003 Å. The obtained bond length R(Cm-O) (2.386 Å) agrees very well with the experimental value (2.32 ± 0.01).[10]

When M^{3+} is extracted by HC301 we have previously reported stable extraction complexes $M(C301)_3$ (M=Eu, Am, Cm),[20] where a C_3 symmetry of the $M(C301)_3$ was determined. In order to estimate the stability of the alternative extraction complexes $M[H(C301)_2]_3$ and $M(C272)_3$ we have taken Cm as an example and calculated the change of the Gibbs free energy ΔG_g^{elec} in the four following reactions:

$$Cm^{3+} + 3(HC272)_2 \longrightarrow Cm[H(C272)_2]_3 + 3H^+ \tag{13}$$

$$Cm^{3+} + \frac{3}{2}(HC272)_2 \longrightarrow Cm(C272)_3 + 3H^+ \tag{14}$$

$$Cm^{3+} + 6(HC301) \longrightarrow Cm[H(C301)_2]_3 + 3H^+ \tag{15}$$

$$Cm^{3+} + 3(HC301) \longrightarrow Cm(C301)_3 + 3H^+ \tag{16}$$

It has been found that for the extractant HC272 the extraction complex $Cm[H(C272)_2]_3$ is formed prior to $Cm(C272)_3$, whereas for the extractant HC301 the $Cm(C301)_3$ complex is most likely preferred, i.e., the calculated ΔG_g^{elec} values at the DFT/BP86 level using basis set B in the equations 13 to 16 are -94.5 kJ/mol, 130.9 kJ/mol, 18.6 kJ/mol, and -9.8 kJ/mol, respectively. The preference of $Cm[H(C272)_2]_3$ over $Cm(C272)_3$ is so strong, that it cannot be reverted by the omitted contributions. A detailed investigation concerning various possible extraction complexes for HC301, where the situation is less clear, is currently underway[52].

By using MOLPRO[36] energy decomposition analyses have been done at the HF level for the model extraction complexes

$M[S_2P(CH_3)_2]_3$ and $M[H(O_2P(CH_3)_2)_2]_3$ (M=Eu, Am, Cm). One can write the electronic interaction energy between two ionic fragments, i.e.,

$$E_{int} = E\big(M[H(O_2P(CH_3)_2)_2]_3\big) - E(M^{3+}) - E\big([H(O_2P(CH_3)_2)_2^-]_3\big) \tag{17}$$

and

$$E_{int} = E\big(M[S_2P(CH_3)_2]_3\big) - E(M^{3+}) - E\big([S_2P(CH_3)_2^-]_3\big) \tag{18}$$

as a sum of three terms

$$E_{int} = E_{ES} + E_{EX} + E_{orb} \ . \tag{19}$$

Here, E_{orb} represents the orbital interaction energy. Based on the converged wavefunctions of two fragments, the initial orbital guess for the molecule, i.e., $M[S_2P(CH_3)_2]_3$ and $M[H(O_2P(CH_3)_2)_2]_3$, is established. The orbital interaction term E_{orb} is extracted from the electronic energy values prior to the first and after the last SCF cycles, e.g., without and with orbital relaxation:

$$E_{orb} = E_{SCF} - E_{0SCF} \tag{20}$$

E_{ES} and E_{EX} denote electrostatic energy and exchange repulsion energy, respectively. They are usually combined together into a single term, E_{steric},

$$E_{steric} = E_{ES} + E_{EX} \ . \tag{21}$$

The calculated orbital and steric contributions to the total interaction energy are shown in Fig. 4. It has been found that the steric contribution (> 70%) plays an important role in the interaction of the metal ion and the ligands. The orbital contributions in $M[S_2P(CH_3)_2]_3$, i.e., 30%, 28%, and 28 % for M=Eu, Cm, and Am, respectively, are slightly larger than those in $M[H(O_2P(CH_3)_2)_2]_3$, i.e., 26% for Eu, 24% for Am, and 25% for Cm. This indicates somewhat stronger covalent interactions of the metal ion M^{3+} and the three $S_2P(CH_3)_2^-$ ligands. This is also consistent with expectations based on chemical intuition, i.e., due to the significantly lower electronegativity of sulfur (2.58, Pauling scale) compared to oxygen (3.44) electrons are more readily shared in a metal-sulfur bond than in a metal-oxygen bond, introducing a greater degree of covalency. Due to the very similar electronegativity values of the metals (Eu 1.2, Am 1.3, Cm 1.3) there are no significant differences between lanthanide and actinide complexes. By means of Mulliken orbital population analyses it has been found that the metals carry less positive charges in $M[S_2P(CH_3)_2]_3$ than in $M[H(O_2P(CH_3)_2)_2]_3$, i.e., the atomic charges on the metal center M=Eu, Am, and Cm are respectively 1.08, 1.21, and 1.19 for $M[S_2P(CH_3)_2]_3$ as well as 1.47, 1.73, and 1.72 for $M[H(O_2P(CH_3)_2)_2]_3$.

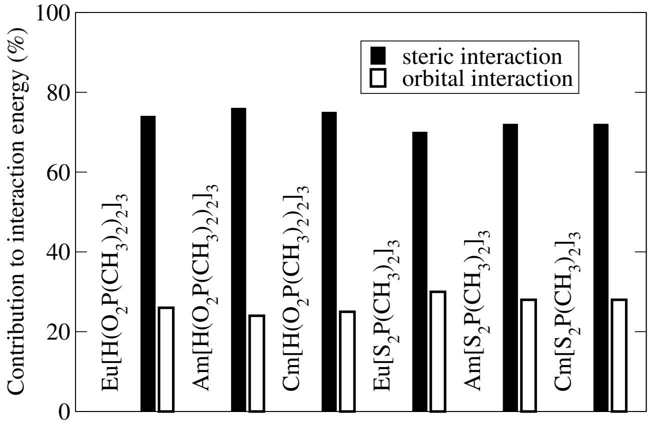

Fig. 4 Decomposition of the total interaction energy in terms of orbital and steric contribution

3.3 Change of the Gibbs Free Energy for M^{3+} + $3(HC272)_2$ → $M[H(C272)_2]_3$ + $3H^+$ (M= Eu, Am, Cm)

For the titled reactions the changes in the Gibbs free energy $\Delta G_{s,e}$=ΔG_g + $\Delta\Delta G_{s,e}$, were calculated for the gas phase (g), for an aqueous solution (s) as well as for the liquid-liquid extraction (e) from the aqueous phase to the organic phase consisting of n-heptane. For the convenience of the discussion we partion the gas phase (ΔG_g) and solvent ($\Delta\Delta G_{s,e}$) contributions further. The gas-phase Gibbs free energy change ΔG_g is split into an electronic contribution and one arising from vibration, rotation and translation:

$$\Delta G_g = \Delta G_g^{elec} + \Delta G_g^{vib+rot+trans} \tag{22}$$

The two contributions are evaluated as follows:

$$\begin{aligned}\Delta G_g^{elec} \quad = \quad & E^{elec}\big(M[H(C272)_2]_3, g\big) \\ & -3E^{elec}\big([HC272]_2, g\big) - E^{elec}(M^{3+}, g)\end{aligned} \tag{23}$$

$$\begin{aligned}\Delta G_g^{vib+rot+trans} \quad = \quad & G_g^{vib+rot+trans}\big(M[H(C272)_2]_3\big) \\ & -3G_g^{vib+rot+trans}\big([HC272]_2\big) \\ & -G_g^{trans}(M^{3+}) + 3G_g^{trans}(H^+)\end{aligned} \tag{24}$$

Note that $E^{elec}(H^+,g)=0$ and thus has been omitted in eqn. 23. The corrections due to the solvents (water, n-heptane) are also split into two parts:

$$\Delta\Delta G_{s,e} = \Delta\Delta G'_{sol} + \Delta\Delta G''_{sol} \tag{25}$$

The neutral extraction complexes $M[H(C272)_2]_3$ as well as HC272 reside for the extraction mainly in the organic (n-heptane) phase ($sol = org$), but are also considered in the aqueous phase ($sol = aqu$), whereas the atomic ions H^+ and M^{3+} are only considered in the aqueous phase:

$$\Delta\Delta G'_{sol} = \Delta G_{sol}\big(M[H(C272)_2]_3\big) - 3\Delta G_{sol}\big([HC272]_2\big) \tag{26}$$

$$\Delta\Delta G''_{aqu} = 3\Delta G_{aqu}(H^+) - \Delta G_{aqu}(M^{3+}) \tag{27}$$

The accurate evaluation of ΔG_s and ΔG_e is hindered by several difficulties and uncertainties, which are well known but cannot be completely removed at present. In our previous study[20] for the separation of Ln^{3+} and An^{3+} by using HC301, it has been proven that the $\Delta G_{s,e}$ evaluated at the PP DFT level produced reasonable trends for Eu^{3+}, Am^{3+}, and Cm^{3+}, but not very accurate absolute $\Delta G_{s,e}$ values. Therefore, for obtaining trends for the three metals

		ΔG_g		$\Delta\Delta G_{s,e}$		
		ΔG_g^{elec} A/B	$\Delta G_g^{vib+rot+trans}$ A/B	$\Delta\Delta G'_{aqu}$ A/B	$\Delta\Delta G'_{org}$ A/B	$\Delta\Delta G''_{aqu}$ cald/estd
HC272						
	Eu	-170.1/-15.2	19.7/	73.6/74.2	26.1/26.1	-6.0/-61.3
	Am	-57.5/107.4	16.3/	73.5/76.4	26.0/26.8	-107.0/-154.5
	Cm	-94.5/73.0	17.2/	73.6/76.5	26.1/26.1	-79.0/-88.5
HC301						
	Eu	-64.2/29.1	10.6/34.5	23.5/33.9	7.3/10.0	-6.0/-61.3
	Am	31.4/118.7	6.3/24.4	26.2/34.2	7.9/9.9	-107.0/-154.5
	Cm	-4.1/85.0	7.6/24.9	26.2/34.8	7.9/10.1	-79.0/-88.5

Table 7 Calculated change in Gibbs free energy components $\Delta\Delta G_g$ and $\Delta\Delta G_{s,e}$ for the reactions M^{3+} + $3(HC272)_2 \rightarrow M[H(C272)_2]_3$ + $3H^+$ and M^{3+} + $3HC301 \rightarrow M(C301)_3$ + $3H^+$ (M=Eu, Am, and Cm) in the gas phase and an aqueous solution and for the extraction with n-heptane for HC272 and kerosene for HC301[a]

[a] .../... refers to the results obtained with basis sets A/B (cf. Tab. 1) for ΔG_g^{elec}, $\Delta G_g^{vib+rot+trans}$, $\Delta\Delta G'_{aqu}$, and $\Delta\Delta G'_{org}$ as well as to quantum chemically derived (Eu^{3+} -3308 kJ/mol[43], Am^{3+} -3207 kJ/mol[44], Cm^{3+} -3235 kJ/mol[44], calcd) and semiempirically estimated[45,46] (estd) values for $\Delta\Delta G''_{aqu}$ of M^{3+}. For H^+, the experimental value $\Delta G_{aqu}(H^+)$=-1104.5 kJ/mol[41] was used in both cases. For the definition of the entries, compare to the text. Dielectric constants: water, 80 (aqu); n-heptane, 1.92 (org for HC272); kerosene, 1.8 (org for HC301). For HC301 data are taken from[20].

we rely on our results of $\Delta G_{s,e}$ obtained at the PP DFT level for reaction eqn. 9. For the monoatomic ions the gas-phase Gibbs free energies at 1 atm and 298.15 K were evaluated using the Sackur-Tetrode equation, i.e., $G_g^{trans}(M^{3+})$ is -44.9, -46.7, and -46.7 kJ/mol for M=Eu, Am, and Cm, respectively, and $G_g^{trans}(H^+)$ is -26.3 kJ/mol. The components of ΔG_g and $\Delta G_{s,e}$ calculated with basis A and B are listed in Tab. 7.

The results of the extraction

$$M^{3+}_{aqu} + 3HL_{org} \rightarrow M(C301)_{3,org} + 3H^+_{aqu} \qquad (28)$$

published in our previous paper[20] relied on a monomer cycle for the calculation of the hydration energies of Eu^{3+}, Am^{3+}, and Cm^{3+}. The corresponding results listed in Tab. 7 are based on a more accurate cluster cycle, which yielded hydration energies of -3308, -3207 and -3235 kJ/mol for Eu^{3+}, Am^{3+}, and Cm^{3+}, respectively[43,44]. In the gas phase using basis set B, the calculated changes in the Gibbs free energy ΔG_g for the formation of the $M[H(C272)_2]_3$ complexes analogous to reaction eqn. 9 are 4.5, 123.8, and 90.2 kJ/mol for M=Eu, Am, and Cm, respectively. The formation of the $M[H(C272)_2]_3$ complexes is thus endergonic, with $Eu[H(C272)_2]_3$ being significantly less unstable than $Am[H(C272)_2]_3$ and $Cm[H(C272)_2]_3$. The corresponding ΔG_g values for the formation of the $M(C301)_3$ complexes analogous to reaction 28 are about 59, 19, and 20 kJ/mol larger for Eu, Am, and Cm, respectively. The quality of the basis sets, especially the metal f functions, is found to have quite big effects on the electronic energy. When going from basis set A to basis set B ΔG_g^{elec} increases by about 155 – 168 kJ/mol for $M[H(C272)_2]_3$ and by about 87 – 93 kJ/mol for $M(C301)_3$.

By taking into account solvent effects, we found that the contributions $\Delta\Delta G'_{aqu}$ from the hydration energies of $(HC272)_2$ and $M[H(C272)_2]_3$ (M=Eu, Am, Cm) increase by at most 3 kJ/mol when going from basis set A to B and are almost identical for Eu, Am, and Cm (74.2 – 76.5 kJ/mol). A similar finding applies to the $\Delta\Delta G'_{org}$ values for the n-heptane phase, which are about a factor of 3 smaller (26.1 – 26.8 kJ/mol) and increase by less than 1 kJ/mol upon basis set extension from A to B. The relative insensitivity of the solvent contributions both towards the basis set quality and the central metal ion were also observed for HC301[20]. In addition the $\Delta\Delta G'_{aqu}$ and $\Delta\Delta G'_{org}$ values for HC301 are not even half as large as for HC272.

Qualitatively, the values for the hydration contributions of the M^{3+} and H^+ cations $\Delta\Delta G''_{aqu}$ exhibit the same trends for the quantum chemically calculated M^{3+} hydration Gibbs free energies, and the semiempirically determined ones, however, the absolute values for a given metal ion differ by 9 – 55 kJ/mol. For HC272 these contributions clearly favor a complex formation for Am^{3+} and Cm^{3+} over the one for Eu^{3+}, but they do not revert the trend of ΔG_g in extraction reaction eqn. 9, which is mainly determined by ΔG_g^{elec}. However in extraction reaction eqn. 28 for HC301 the more negative Gibbs free hydration energy for Eu^{3+} compared to Am^{3+} and Cm^{3+} reverts the trend of ΔG_g, cf. Tab. 8.

The change of Gibbs free energies ΔG_s for reaction eqn. 9 and reaction eqn. 28 in aqueous solution as well as ΔG_e for an extraction with n-heptane for HC272 and kerosene for HC301 are shown in Tab. 8. Because the actual mechanism of the extraction process, which was suggested by experimentalists to occur probably mainly at the boundary between the aqueous and organic phases for HC272[53], is too complex to be studied by quantum chemical methods, we only try to model the situation before (M^{3+} in water, $(HC272)_2$ in n-heptane and HC301 in kerosene) and after (3 H^+ in water, $M[H(C272)_2]_3$ in n-heptane and $M(C301)_3$ in kerosene) the extraction and omit kinetic aspects. It is worthwhile to mention here that it has been found by Modolo and Odoj[9] that at room temperature the extraction equilibrium for Am^{3+} over Eu^{3+} by using purified Cyanex301 was already attained within 5 minutes.

ΔG_e for the extraction is consistently lower than ΔG_s for the aqueous solution, in agreement with the experimental finding that $M[H(C272)_2]_3$, $M(C301)_3$, HC272, and HC301 mainly reside in the organic phase. For HC272 the obtained ΔG_s and ΔG_e for Eu^{3+} are at least 20 kJ/mol smaller than those for Am^{3+} and Cm^{3+}. Therefore it is concluded that HC272 prefers Eu^{3+} over Am^{3+} and Cm^{3+}. On the other hand for HC301 the obtained ΔG_s and ΔG_e values for Eu^{3+} are at least 10 kJ/mol larger than those for Am^{3+} and Cm^{3+}. Thus HC301 is expected to prefer Am^{3+} and Cm^{3+} over Eu^{3+}. The calculated thermodynamical priorities, i.e., HC272 for Eu^{3+} and HC301 for Am^{3+} and Cm^{3+}, agree with the

	ΔG_s		ΔG_e	
	calcd A/B	estd A/B	calcd A/B	estd A/B
HC272				
Eu	-82.9/72.7	-111.9/17.4	-130.4/24.6	-185.7/-30.7
Am	-74.7/93.2	-122.7/45.7	-122.2/43.6	-170.2/-3.9
Cm	-82.7/87.7	-92.7/78.2	-130.3/37.3	-140.3/27.8
HC301				
Eu	-35.6/92.0	-91.4/36.2	-51.8/68.1	-107.6/12.3
Am	-42.6/70.8	-90.6/22.8	-60.9/46.5	-108.9/-1.5
Cm	-48.8/66.2	-58.8/56.5	-67.1/41.5	-77.1/31.5

Table 8 Calculated change of the Gibbs free energy for the reactions M^{3+} + 3(HC272)$_2$ → M[H(C272)$_2$]$_3$ + 3H$^+$ and M^{3+} + 3HC301 → M(C301)$_3$ + 3H$^+$ (M=Eu, Am, Cm) in aqueous solution (ΔG_s) and for the liquid-liquid extraction (ΔG_e)[a]

[a] .../... refers to the results obtained with basis sets A/B (cf. Tab. 1). Individual contributions cf. Tab. 7. As organic phase n-heptane and kerosene were assumed for HC272 and HC301, respectively. Quantum chemically derived (calcd) as well as semiempirically estimated (estd) values for $\Delta\Delta G''_{aqu}$ of M^{3+} were used. For H$^+$, the experimental value $\Delta G_{aqu}(H^+)$=-1104.5 kJ/mol was used in both cases.

experimental observations.[4,5] For HC301 the results using basis set B obtained with quantum chemically derived values for the Eu^{3+} and Am^{3+} Gibbs free hydration energies, i.e., 68.1 kJ/mol for Eu and 46.5 kJ/mol for Am, agree very well with the estimated experimental values (63.3 kJ/mol for Eu and 44.1 kJ/mol for Am[5]). The value for Cm is close to the one for Am as expected, i.e., ΔG_s and ΔG_e for Cm^{3+} obtained with quantum chemically derived values are at most 5 kJ/mol lower than for Am^{3+}.

Recently, based on the optimized geometries at the MP2 level for Ln^{3+} and at the DFT/BP86 level for An^{3+}, single-point calculations using aug-cc-pVTZ basis sets at the CCSD(T) level by means of the incremental scheme have been carried out for $[M^{3+}(H_2O)_h]$ complexes (M=Ln, An; h=8, 9) to obtain the Gibbs free hydration energies for lanthanoid(III)[54] and actinoid(III)[55] ions. The CCSD(T) values (Eu^{3+} -3386 kJ/mol; Am^{3+} -3281 kJ/mol; Cm^{3+} -3309 kJ/mol) for coordination number 9 and derived from a cluster cycle are by 74 – 78 kJ/mol lower than the corresponding MP2 results (Eu^{3+} -3308 kJ/mol[43]; Am^{3+} -3207 kJ/mol[44]; Cm^{3+} -3235 kJ/mol[44]). Applying these CCSD(T) data the ΔG_e values for Eu^{3+}, Am^{3+} and Cm^{3+} become 97.6, 117.6, and 111.3 kJ/mol for HC272 and 141.1, 120.2, and 115.5 kJ/mol for HC301, respectively. Whereas the trend of the results based on MP2 hydration energies is kept, the agreement of the absolute values with the experimental ones is somewhat worse. Unfortunately, at present it is not possible to perform CCSD(T) calculations for the extraction complexes using aug-cc-pVTZ basis sets in order to derive pure CCSD(T) results. Replacing the quantum chemically calculated Gibbs free hydration energies for Eu^{3+}, Am^{3+}, and Cm^{3+} by semiempirically estimated values (Eu^{3+} -3252 kJ/mol[45], Am^{3+} -3159 kJ/mol[46], Cm^{3+} -3225 kJ/mol[46]) the values for ΔG_e are -30.7, -3.9, and 27.8 kJ/mol for HC272, and 12.30, -1.5, and 31.5 kJ/mol for HC301, respectively. Whereas for Eu^{3+} and Am^{3+} the experimentally observed preference of the extraction with HC272 and HC301, respectively, is in line with these results, the values for Cm^{3+} do not reflect the preference for an extraction with HC301.

4 Conclusions

The widely used extractants HC272 (Cyanex272) and HC301 (Cyanex301) as well as their dimers have been studied using the DFT/BP86 and MP2 methods. It has been found that HC272 exists primarily as self-associated species as a result of hydrogen bonding, whereas HC301 preferably exists as monomer. Moreover the calculations for small model systems of extractants, i.e., $[O_2HP(CH_3)_2]_n$ and $[S_2HP(CH_3)_2]_n$ (n=1-4), yielded a negative change of the Gibbs free energy for the reactions $n[HO_2P(CH_3)_2] \rightarrow [HO_2P(CH_3)_2]_n$ (n=2,3,4), and thus imply that the degree of aggregation of the extractant HC272 might reach three or even higher.

The experimentally observed opposite selectivity of HC272 and HC301 on Eu^{3+} and Am^{3+} has been studied and correctly obtained at the DFT/BP86 level in connection with scalar-relativistic energy-consistent 4f/5f-in-core lanthanide/actinide PPs. For the neutral extraction complexes M[H(C272)$_2$]$_3$ and M(C301)$_3$, the metal cation is coordinated by six O atoms for HC272 and by six S atoms for HC301, respectively. The M-O(S) bond distances do reflect the cation employed, i.e., the larger the cation, the longer the bond. The calculated M-O/M-S bond lengths (Eu: 2.337/2.841Å; Am: 2.403/2.900 Å; Cm: 2.386/2.883 Å) agree well with the available experimental data [R(Cm-O)=2.32 ± 0.01 Å; R(Cm-S)=2.826 ± 0.008 Å]. Moreover the studies on Cm(C272)$_3$ and Cm[H(C301)$_2$]$_3$ by calculating the changes of the Gibbs free energies in reactions 13 and 14 have shown that the extraction complexes M[H(C272)$_2$]$_3$ are formed prior to M(C272)$_3$, whereas for HC301 it is the other way round, i.e., M(C301)$_3$ is preferred. An energy decomposition analysis for model extraction complexes $M[S_2P(CH_3)_2]_3$ and $M[H(O_2P(CH_3)_2)_2]_3$ (M=Eu, Am, Cm) has shown that the steric contribution (>70%) plays an important role in the interaction between metal ion and ligands. Moreover a stronger covalent interaction between metal ion M^{3+} and ligands has been found for $[S_2P(CH_3)_2^-]_3$ than for $[H(O_2P(CH_3)_2)_2^-]_3$. The changes of the Gibbs free energy, ΔG, in the reactions M^{3+} + 3(HC272)$_2$ → M[H(C272)$_2$]$_3$ + 3H$^+$ and M^{3+} + 3(HC301) → M(HC301)$_3$ (M= Eu, Am, Cm) in the gas phase and aqueous solution and for extraction from aqueous solution with n-heptane for HC272 and kerosene for HC301 have been studied too. It has been found that the electronic energy differences between the reactants and products play an important role for the selectivity of HC272 for Eu^{3+} over Am^{3+}. In the gas phase the calculated value of ΔG_g for Eu^{3+} (4.5 kJ/mol) is significantly smaller than those for Am^{3+} (123.8 kJ/mol) and Cm^{3+} (90.2 kJ/mol), and this order is kept for the aqueous solution (ΔG_s: Eu^{3+} 72.7 kJ/mol; Am^{3+} 93.2 kJ/mol; Cm^{3+} 87.7 kJ/mol) as well as for the extraction (ΔG_e: Eu^{3+} 24.6 kJ/mol; Am^{3+} 43.6 kJ/mol; Cm^{3+} 37.3 kJ/mol). For HC301 the calculated gas phase ΔG_g value for Eu^{3+} (63.6 kJ/mol) is smaller than those for Am^{3+} (143.1 kJ/mol) and Cm^{3+} (109.9 kJ/mol), whereas this order is reverted for the aqueous solution (ΔG_s: Eu^{3+} 92.0 kJ/mol; Am^{3+} 70.8 kJ/mol; Cm^{3+} 66.2 kJ/mol) as well as for the extraction (ΔG_e: Eu^{3+} 68.1 kJ/mol; Am^{3+} 46.5 kJ/mol; Cm^{3+} 41.5 kJ/mol) due to the lower hydration Gibbs free energy for Eu^{3+} (-3308 kJ/mol)[43] comparing to Am^{3+} (-3207 kJ/mol)[44] and Cm^{3+} (-

3235 kJ/mol)[44]. The absolute values ΔG_e (Eu^{3+} 68.1 kJ/mol; Am^{3+} 46.5 kJ/mol) agree quite well with the the experimental findings (Eu^{3+} 63.3 kJ/mol; Am^{3+} 44.1 kJ/mol)[5]. Applying recently published hydration Gibbs free energies for Eu^{3+} (-3386 kJ/mol)[55] and Am^{3+} (-3281 kJ/mol)[55] calculated at the CCSD(T) level by means of the incremental scheme, the obtained absolute values (Eu^{3+} 141.1 kJ/mol; Am^{3+} 120.2 kJ/mol) disagree within 80 kJ/mol with the experimental data, whereas the correct trend is kept. Accurate correlated ab initio reference calculations for the extraction complexes, as well as further experiments on trivalent lanthanide and especially actinide aquo ions, should be conducted in the future in order to get besides more accurate values for M^{3+} hydration Gibbs free energies also more reliable data needed for the evaluation of the energetics of the whole extraction processes.

Acknowledgement

X.C. is grateful to the German Science Foundation (Deutsche Forschungsgemeinschaft, DFG) for support.

References

1 G. Tian, Y. Zhu, J. Xu, P. Zhang, T. Hu, Y. Xie, J. Zhang, *Inorg. Chem.* 2003, **42**, 735-741.

2 P. J. Panak, A. Geist, *Chem. Rev.* 2013, **113**, 1199-1236.

3 K. L. Nash, In: *Handbook of Chemistry and Physics of Rare Earths*, K. A. Gschneidner, L. Eyring, G. R. Choppin, G. H. Lander (Eds.) vol. 18, p. 197, Elsevier, New York, 1994.

4 Y. Zhu, C. Song, R. Jiao, *Global 95 International Conference on Evaluation of Emerging Nuclear Fuel Cycle System*, Versailles, France, Sept. 11–14., pp 571–576, 1995.

5 Y. Zhu, J. Chen, R. Jiao, *Solvent. Extr. Ion. Exch.* 1996, **14**, 61-68.

6 J.-M. Nan, D.-M. Han, X.-X. Zou, *J. Power Sources* 2005, **1**, 278-284.

7 J.-M. Nan, D.-M. Han, M.-J. Yang, M. Cui, X.-L. Hou, *Hydrometallurgy* 2006, **84**, 75-80.

8 T. Hirai, T. Orikoshi, I. Komasawa, *Chem Mat.* 2002, **14**, 3576-3583.

9 G. Modolo, R. Odoj, *J. Radioanal. Nucl. Chem.* 1998, **228**, 83-88.

10 M. P. Jensen, A. H. Bond, *J. Am. Chem. Soc.* 2002, **124**, 9870-9877.

11 M. P. Jensen, A. H. Bond, *Radiochim. Acta* 2002, **90**, 205-209.

12 C. Hill, In: *Ion Exchange and Solvent Extraction*; B. A. Moyer (Ed.), CRC Press, Boca Raton/London/New York, 2010, Vol. 19.

13 M. Dolg, X. Cao, *Chem. Rev.* 2012, **112**, 403-480.

14 M. Dolg, H. Stoll, A. Savin, H. Preuss, *Theor. Chim. Acta* 1989, **75**, 173-194.

15 M. Dolg, H. Stoll, H. Preuss, *Theor. Chim. Acta* 1993, **85**, 441-450.

16 M. Dolg, H. Stoll, H. Preuss, *J. Chem. Phys.* 1989, **90**, 1730-1734.

17 W. Küchle, M. Dolg, H. Stoll, H. Preuss, *J. Chem. Phys.* 1994, **100**, 7535-7542.

18 A. Moritz, X. Cao, M. Dolg, *Theor. Chem. Acc.* 2007, **118**, 845-854.

19 A. Moritz, X. Cao, M. Dolg, *Theor. Chem. Acc.* 2007, **117**, 473-481.

20 X. Cao, D. Heidelberg, J. Ciupka, M. Dolg, *Inorg. Chem.* 2010, **49**, 10307-10315.

21 M. Dolg, X. Cao, J. Ciupka, *J. Electron. Spectrosc. Relat. Phenom.* 2014, **194**, 8-13.

22 J. Yang, M. Dolg, *Theor. Chem. Acc.* 2005, **113**, 212-224.

23 M. Dolg, *J. Chem. Theory Comput.* 2011, **7**, 3131-3142.

24 J.-H. Lan, W.-Q. Shi, L.-Y. Yuan, J. Li, Y.-L. Zhao, Z.-F. Chai, *Coord. Chem. Rev.* 2012, **256**, 1406£1417.

25 A. Klamt, G. Schüürmann, *J. Chem. Soc. Perkin Trans.* 1993, **2**, 799-805.

26 TURBOMOLE is a program package developed by the Quantum Chemistry Group at the University of Karlsruhe, Germany, since 1988. R. Ahlrichs, M. Bär, M. Häser, H. Horn, C. Kölmel, *Chem. Phys. Lett.* 1989, **162**, 165-169.

27 Unpublished; TURBOMOLE basis set library.

28 A. Schäfer, H. Horn, R. Ahlrichs, *J. Chem. Phys.* 1992, **97**, 2571-2577.

29 A. Weigand, X. Cao, J. Yang, M. Dolg, *Theor. Chem. Acc.* 2009, **126**, 117-127.

30 F. Weigend, M. Häser, H. Patzelt, R. Ahlrichs, *Chem. Phys. Lett.* 1998, **294**, 143-152.

31 F. Weigend, R. Ahlrichs, *Phys. Chem. Chem. Phys.* 2005, **7**, 3297-3305.

32 A. Hellweg, C. Hättig, S. Höfener, W. Klopper, *Theor. Chem. Acc.* 2007, **117**, 587-597.

33 F. Weigend, M. Häser, *Theor. Chem. Acc.* 1997, **97**, 331-340.

34 A. D. Becke, *Phys. Rev. A* 1988, **38**, 3098-3100.

35 J. P. Perdew, *Phys. Rev. B* 1986, **33**, 8822-8824.

36 http://www.molpro.net (accessed May 28, 2015).

37 J. Zhang, M. Dolg, *J. Chem. Theory Comput.* 2013, **9**, 2992-3003.

38 J. Zhang, M. Dolg, *J. Chem. Phys.* 2014, **140**, 044114-1-9.

39 J. Zhang, M. Dolg, *J. Chem. Theor. Comput.* 2015, **11**, 962-968.

40 T. H. Dunning, Jr., *J. Chem. Phys.* 1989, **90**, 1007-1023.

41 M. D. Tissandier, K. A. Cowen, W. Y. Feng, E. Gundlach, M. H. Cohen, A. D. Earhart, T. R. Tuttle, J. V. Coe, *J. Phys. Chem. A* 1998, **102**, 7787-7794.

42 S. Goldman, L. R. Morss, *Can. J. Chem.* 1975, **53**, 2695-2700.

43 J. Ciupka, X. Cao-Dolg, J. Wiebke, M. Dolg, *Phys. Chem. Chem. Phys.* 2010, **12**, 13215-13223.

44 Ciupka, J.: personal communication

45 F. H. David, V. Vokhmin, G. Ionova, *J. Mol. Liq.* 2001, **90**, 45-62.

46 F. H. David, V. Vokhmin, *New J. Chem.* 2003, **27**, 1627-1632.

47 D. M. Camaioni, C. A. Schwerdtfeger, *J. Phys. Chem. A* 2005, **109**, 10795-10797.

48 C. P. Kelly, C. J. Cramer, D. G. Truhlar, *J. Phys. Chem. B* 2006, **110**, 16066-16081.

49 K. C. Sole, J. B. Hiskey, *Hydrometallurgy* 1995, **37**, 129-147.

50 N. A. Grigorieva, N. I. Pavlenko, M. A. Pleshkov, G. L. Pashkov, I. Yu. Fleitlikh, *Solvent Extr. Ion. Exch.* 2009, **27**, 745-760.

51 S. F. Boys, F. Bernardi, *Mol. Phys.* 1970, **19**, 553-566.

52 Weissmann, D. *doctoral thesis*, University of Cologne, 2015.

53 N. Rahman, J. A. Daoud, H. F. Aly, *J. Radioanal. Nucl. Chem.* 2003, **25**, 597-603.

54 J. Zhang, N. Heinz, M. Dolg, *Inorg. Chem.* 2014, **53**, 7700-7708.

55 N. Heinz, J. Zhang, M. Dolg, *J. Chem. Theory Comput.* 2014, **10**, 5593-5598.